On the Observed Annual Cycle in the Ocean-Atmosphere Heat Balance Over the Northern Hemisphere

ABRAHAM H. OORT

Geophysical Fluid Dynamics Laboratory/NOAA, Princeton University, Princeton, N. J. 08540

THOMAS H. VONDER HAAR

Department of Atmospheric Science, Colorado State University, Fort Collins, Colo. 80523

(Manuscript received 22 March 1976, in revised form 1 July 1976)

ABSTRACT

Based on the best presently available satellite radiation, atmospheric and oceanic data sets the long-term mean heat balance of the earth and its normal seasonal variation are investigated over the Northern Hemisphere. Quantitative estimates for the various flux and storage terms in the atmospheric and terrestrial branches of the heat balance are given for 10° wide latitude belts and for each calendar month. The results are presented in both graphical and tabular form. As was known before, the storage of heat in the oceans is found to dominate the energy storage in the combined atmosphere-ocean-land-cryosphere system. In the tropics, large changes in oceanic heat storage are found in the 10°N–20°N belt with a maximum in spring and a minimum in late summer. The main new finding of this study is that the inferred oceanic heat transports appear to undergo very large seasonal variations especially in the tropics. Between 10°N and 20°N, maximum northward oceanic transports of 4 to 5×10^{15} W were computed in spring and late fall, which are as large as or larger than the corresponding mid-latitude atmospheric transports. Near the equator the oceanic fluxes were found to reverse seasonally and be directed generally toward the winter hemisphere with an absolute maximum of -8×10^{15} W in August.

1. Introduction

It is common knowledge that the atmospheric and oceanic circulations play a significant role in the climatic picture of the earth. Without them, local radiative equilibrium would predominate, and the climate everywhere on the globe would be much harsher than it is presently observed. The moderating influence of the atmosphere and oceans, in general, is twofold. First of all, the oceans and to a lesser degree the atmosphere serve as reservoirs where large amounts of energy are stored during summer and released during winter. These effects thereby cause a substantial reduction of the winter-summer differences in a radiatively controlled climate. In the second place, the atmospheric and oceanic circulations transport large amounts of energy from warm to cold regions, leading to a spatial smoothing of the climate.

In an earlier study (Vonder Haar and Oort, 1973) it was found that the atmospheric and oceanic transports are of comparable overall importance, at least on an annual basis. The oceans seem to accomplish the major transport at low latitudes, while the atmosphere takes care of the transport at middle and high latitudes. The low-latitude oceanic contribution was found to be almost twice as large as in previous studies. The present study deals with the annual variation in these heat fluxes. This new dimension in time will bring up the first climatic aspect of the atmosphere and oceans mentioned above, namely, their role in storing heat. It is well known (e.g., Gabites, 1950) that the oceans are highly effective in smoothing the seasonal cycle because of their enormous heat capacity and large coverage over the globe. The atmosphere, land and cryosphere also contribute, but much less, the first two because of their smaller effective heat capacity and the ice and snow because of the minor seasonal variations in their horizontal and vertical extent.

For earlier work along these lines, see Gabites (1950), Rasool and Prabhakara (1966), Newell *et al.* (1970, 1974), Fritz (1958) and Pattullo (1957). Several years of global satellite radiation data, as well as global atmospheric and oceanic data, have recently become available and justify now a new look at the fundamental balances determining the earth's climate.

One of the least known parameters in the climate problem, as was discussed in our previous paper, is the oceanic heat flux. The most obvious and straightforward approach to obtain estimates of this heat flux would be, as has been done in the atmosphere, to measure it directly *in situ*. Thus, one would have to monitor simultaneously the velocity and temperature fields in the world oceans throughout the year. How-

ever, except for some limited, local velocity measurements, practically no data are available to describe the three-dimensional velocity fields in the oceans. Obvious reasons for this deficiency include the difficulties in measuring the velocity from a moving ship or buoy, the enormous area to be covered, the accuracy needed to measure the relatively slow but important motions in the deep ocean, the occurrence of mesoscale eddies that would necessitate long time series and high spatial resolution to get representative fluxes, etc. Thus, the direct approach cannot be expected to yield any representative heat flux values for the world oceans in the near future. For the time being, one must resort to some indirect method. Some of the indirect methods are listed and discussed below.

1) From general heat balance considerations of the entire atmosphere-ocean-earth system one can estimate as a residual the local convergence of heat by ocean currents (Vonder Haar and Oort, 1973). This method will also be used in the present study.

2) From heat balance considerations at the ocean surface, one can make similar attempts (e.g., Budyko, 1963; Bryan and Schroeder, 1960; Bryan, 1962).

3) In the oceans one may estimate the stationary component of the heat flux using both observed mean temperatures and calculated geostrophic velocities. These velocities could be derived from the observed three-dimensional density fields as was done for the annual mean conditions over the North Atlantic Ocean by Holland and Hirschman (1972).

4) Finally, in numerical experiments with a very high resolution grid one should be able not only to calculate the model heat fluxes, but also to evaluate the relative importance of mean flow and eddies in the overall oceanic heat balance.

In the present study, the general problem of the earth's heat budget will be discussed on a mean monthly basis. Emphasis will be on the mean, steady-state solution. The estimates to be presented here are based on, we believe, the most comprehensive net radiation, atmospheric and oceanic data sets presently available. This effort will hopefully lay bare what is known about the earth's heat budget, how well it is known, what is not known, and what should be done to fill the gaps. The determination of each term in the heat balance has, of course, its own particular difficulties. Included among these is the non-simultaneity of the different data sets. Therefore, an Appendix has been added to this paper where the probable errors in each estimate are presented and discussed.

2. Formulation of the problem

The theoretical framework needed for the present analyses will be based on the physical law of conservation of energy. This law will be applied both to the combined atmosphere-ocean-land-cryosphere system as well as to the atmosphere and the remainder of the system separately (we will often call this remainder, for convenience, the "earth"). Through this procedure, one may expect to learn more about the nature of the energy exchanges not only within the different media but also between them. A somewhat similar approach was used before by Newell *et al.* (1974). The only difference with their approach is that in the present formulation water vapor is treated explicitly as a form of latent energy, while Newell *et al.* considered the effects of water vapor only when condensation (heating) or evaporation (cooling) takes place.

The symbols used are listed in the Appendix. Vertical integration limits will be indicated by the letters T and B for top and bottom, followed by a letter indicating the medium considered.

The first step will be to write down the balance equation of energy for a vertical column of unit area cross section throughout the entire vertical extent of the atmosphere-earth system [the vertical integration in the case of land and ocean is assumed to be carried out down to the depth of penetration of the annual variation (for the oceans a uniform depth of 275 m is assumed in Section 4b)]:

$$\frac{\partial E}{\partial t}=F_{\mathrm{TA}}-\operatorname{div}\mathbf{T}_{\mathrm{A}}-\operatorname{div}\mathbf{T}_{\mathrm{O}}, \tag{1}$$

where

$$\frac{\partial E}{\partial t}=S_{\mathrm{A}}+S_{\mathrm{O}}+S_{\mathrm{L}}+S_{\mathrm{I}} \tag{1a}$$

$$S_{\mathrm{A}}=\frac{\partial}{\partial t}\int_{\mathrm{BA}}^{\mathrm{TA}}\rho(C_{\mathrm{A}}T+gZ+L_e q)dz \tag{1b}$$

$$S_{\mathrm{O}}=\frac{\partial}{\partial t}\int_{\mathrm{BO}}^{\mathrm{TO}}\rho C_{\mathrm{O}}T\,dz \tag{1c}$$

$$S_{\mathrm{L}}=\frac{\partial}{\partial t}\int_{\mathrm{BL}}^{\mathrm{TL}}\rho C_{\mathrm{L}}T\,dz \tag{1d}$$

$$S_{\mathrm{I}}=\frac{\partial}{\partial t}\int_{\mathrm{BI}}^{\mathrm{TI}}\rho(C_{\mathrm{I}}T-L_m)\,dz \tag{1e}$$

F_{TA} = net flux of radiation at top of the atmosphere (incoming shortwave minus reflected shortwave and outgoing longwave) (1f)

$$\operatorname{div}\mathbf{T}_{\mathrm{A}}=\nabla_2\cdot\int_{\mathrm{BA}}^{\mathrm{TA}}\rho\left(C_{\mathrm{A}}T+\frac{p}{\rho}+gZ+L_e q\right)\mathbf{V}\,dz \tag{1g}$$

$$\operatorname{div}\mathbf{T}_{\mathrm{O}}=\nabla_2\cdot\int_{\mathrm{BO}}^{\mathrm{TO}}\rho\left(C_{\mathrm{O}}T+\frac{p}{\rho}+gZ\right)\mathbf{V}\,dz. \tag{1h}$$

The appropriate conservation law of energy for the atmosphere alone, or what may be called in analogy with the usage in hydrology (e.g., Peixóto, 1973), the "atmospheric branch" of the energy cycle, may be written in the form

$$S_A = F_{TA} - F_{BA} - \text{div}\mathbf{T}_A, \tag{2}$$

where in addition to the already explained terms

$$F_{BA} = F_{BA}^{R} + F_{BA}^{SH} + F_{BA}^{LH}$$
$$= \text{net flux of energy (radiation + sensible heat + latent heat) from atmosphere to earth.} \tag{2a}$$

Finally, the conservation equation for the "terrestrial branch" of the energy cycle is written as

$$S_O + S_L + S_I = F_{BA} - \text{div}\,\mathbf{T}_O. \tag{3}$$

For clarity, a schematic diagram showing the different energy terms in the atmospheric and terrestrial branches of the energy cycle is given in Fig. 1. Further, it should be said here that (1), (2) and (3) are not fully complete, since certain effects, such as the release of geothermal energy and the transport of latent heat in icebergs, have been left out. However, these missing terms are insignificant for the present problem. We will see later that even the terms retained are not all equally important. Thus, it will turn out that the energy storage in the land S_L can also be neglected in (1) and (3).

Up to this point, the conservation equations have been written for a particular instant of time and a vertical column of atmospheric and terrestrial mass with a unit area cross section. For later use, the following averaging operators in time and space will be introduced:

$$\bar{F} = \int_{t_1}^{t_2} F\,dt \Big/ (t_2 - t_1), \tag{4}$$

$$\langle F \rangle = \int\int_A F\,a^2 \cos\phi\, d\lambda\, d\phi \Big/ \int\int_A a^2 \cos\phi\, d\lambda\, d\phi, \tag{5}$$

where F is an arbitrary variable, A an arbitrary area on the globe, t the time, a the radius of the equivalent spherical earth, λ the longitude, and ϕ the latitude. Thus, (1), (2) and (3) can be written in averaged form as follows:

$$\langle \bar{S}_A \rangle + \langle \bar{S}_O \rangle + \langle \bar{S}_L \rangle + \langle \bar{S}_I \rangle = \langle \bar{F}_{TA} \rangle - \langle \text{div}\,\overline{\mathbf{T}}_A \rangle - \langle \text{div}\,\overline{\mathbf{T}}_O \rangle \tag{6}$$

$$\langle \bar{S}_A \rangle = \langle \bar{F}_{TA} \rangle - \langle \bar{F}_{BA} \rangle - \langle \text{div}\,\overline{\mathbf{T}}_A \rangle \tag{7}$$

$$\langle \bar{S}_O \rangle + \langle \bar{S}_L \rangle + \langle \bar{S}_I \rangle = \langle \bar{F}_{BA} \rangle - \langle \text{div}\,\overline{\mathbf{T}}_O \rangle. \tag{8}$$

The conservation equations in the integrated form (6), (7) and (8) with real data will be used in the following sections to evaluate the different energy components in the earth's heat budget. Since our present interest lies in clarifying the role of the annual cycle in the large-scale heat balance, the basic time and space units for averaging have been chosen as *one month* and a *zonal belt with a width of 10° latitude.*

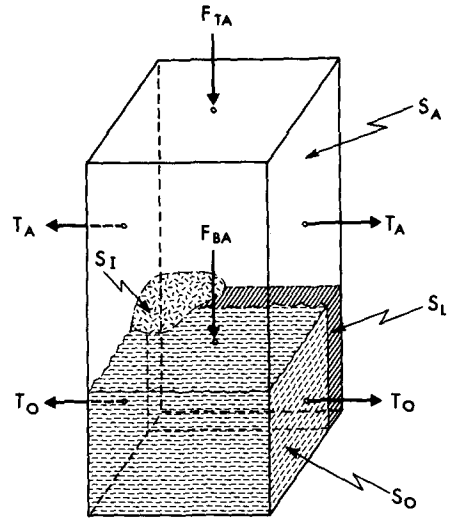

FIG. 1. Schematic diagram of the different terms in the earth's energy balance.

There are three different categories of data that will be used to calculate the various terms appearing in (6), (7) and (8). These categories are net radiation data from satellites, atmospheric data from radiosonde balloons, and oceanic data taken from ships. The radiation data supply estimates of F_{TA}, the atmospheric data S_A and div $\mathbf{T}_A$, while the oceanic data give estimates of S_O. Assuming that S_L and S_I can be neglected (see Section 4b), one can then calculate the two unknown quantities, F_{BA} and div $\mathbf{T}_O$ from (7) and (8).

The exchange of energy between the atmosphere and the underlying earth's surface, F_{BA}, cannot be measured directly. It has up to now only been evaluated in a very crude manner by estimating the three individual components F_{BA}^{R}, F_{BA}^{SH} and F_{BA}^{LH} separately from other climatological data (see, e.g., the atlas by Budyko, 1963). The present method will supply independent and perhaps more reliable estimates of this important term, at least on a zonal mean basis.

The horizontal divergence and convergence by oceanic motions (slow drifts, currents and eddies combined) seems to be almost impossible to estimate by conventional methods. As mentioned before, the present approach may prove to be perhaps the only practical way to estimate the large-scale oceanic transports from observations.

In summary, the new results to be provided here are monthly estimates of $\langle \bar{F}_{BA} \rangle$, $\langle \text{div}\,\overline{\mathbf{T}}_O \rangle$ and $\langle \overline{\mathbf{T}}_O \rangle$.

3. The basic data

The observations used in the present paper were taken from satellites, ground stations and oceano-

graphic ships during the last two decades. Much of the processing of the observations was done at various universities and governmental institutions. However, the final evaluation to obtain reliable estimates of the earth's heat balance still requires a major data reduction effort on the part of the scientists involved. Thus, the final collection and assembly into means of the satellite data was done at the Department of Atmospheric Science of Colorado State University. Processing of the atmospheric data was accomplished in the early 70's in cooperation with Professor V. P. Starr's MIT Planetary Circulations Project at the Geophysical Fluid Dynamics Laboratory (GFDL) in Princeton, N. J., while the oceanic data were also analyzed at GFDL.

The first basic data set used consists of reflected solar and infrared radiation measurements from earth-orbiting satellites taken during the years 1964 through 1971. The albedo measurements of the atmosphere-earth system gave the information needed to calculate the incoming, solar radiation, assuming a solar constant of 1360 W m^{-2}. Combined with simultaneous measurements of outgoing infrared radiation, the net radiation balance at the top of the atmosphere, F_{TA}, was evaluated on a monthly basis. For most satellite sensors, the ground resolution was low, of the order of 1000 km $\times$1000 km. In view of this lower limit of resolution, all energy budget terms will be presented here only for 10° latitude wide zones. More detailed information on the satellite data that have been included in the present study, as well as the sample size in terms of months and years, and the local time of observation is presented in Table 1. The table shows that the number of individual yearly samples for each calendar month is generally small, only on the order of 2 or 3. All satellites were in sun-synchronous orbits, thus sampling at just one local time during daylight hours. However, the 29 month set includes both late morning, near noon and early afternoon orbits so that diurnal sampling bias is minimized. For further information concerning the satellite data the reader is referred to MacDonald (1970), Vonder Haar and Suomi (1971), Flanders and Smith (1975), and Ellis and Vonder Haar (1976).

The second data set is based on a large sample of daily aerological reports from about 600 Northern Hemisphere stations for the period May 1958 through April 1963. It contains monthly mean, three-dimensional distributions of the temperature $\bar{T}$, geopotential height $\bar{Z}$, specific humidity $\bar{q}$, and their horizontal transports $\overline{V}\overline{T}$, $\overline{V}\overline{Z}$ and $\overline{V}\overline{q}$. An objective analysis scheme with a zonal average of the data as a first guess field, was used to interpolate the monthly mean values from the station network to a regular polar stereographic grid. These analyses were carried out for each parameter, each calendar month, and for 11 levels between 1000 and 50 mb height. For further information concerning this data set the reader is referred to Oort and Rasmusson (1971). Vertical intergration of the quantity $(C_A\bar{T}+g\bar{Z}+L_e\bar{q})$ over the atmospheric mass between the earth's surface and 75 mb gave an estimate of the energy stored in the atmosphere. The rate of energy storage, S_A, was then obtained by subtracting the estimates for consecutive months. The horizontal monthly mean transports of atmospheric energy, $\mathbf{T}_A$, were finally obtained through vertical integration of the quantity $(c_p\overline{T}\overline{\mathbf{V}}+g\overline{Z}\overline{\mathbf{V}}+L_e\overline{q}\overline{\mathbf{V}})$. The resulting values include the transports by both time-mean flow, as well as those by the transient and stationary eddies.

Finally, the third data set is based on all historical hydrographic station data (about 400,000 casts) and bathythermograph records (about 700,000) available at NOAA's National Oceanographic Data Center, as of June 1973. For each 1°$\times$1° ocean square in the Northern Hemisphere all available temperature data for a particular calendar month were first crudely checked

TABLE 1. Chronological list of earth-orbiting satellites from which the present radiation measurements were taken. The approximate local time at which each satellite crossed the equator during daylight hours is given in parentheses. EX = Experimental, N2 = Nimbus 2, N3 = Nimbus 3, E7 = ESSA 7, I1 = ITOS 1, and NO1 = NOAA 1.

Months	Year 1964	1965	1966	1967	1968	1969	1970	1971	Sample size
Jan		EX (10:30)				E7 (14:30)	N3 (11:30)		3
Feb		EX (10:35)				E7 (14:30)			2
Mar		EX (10:40)				E7 (14:30)			2
Apr						N3 (11:30)	I1 (15:00)		2
May			N2 (11:30)			N3 (11:30)	I1 (15:00)	NO1 (15:00)	4
Jun			N2 (11:30)			N3 (11:30)	I1 (15:00)		3
Jul	EX (08:30)		N2 (11:30)			N3 (11:30)			3
Aug	EX (08:55)					N3 (11:30)			2
Sep	EX (09:15)								1
Oct	EX (09:40)				E7 (14:30)	N3 (11:30)			3
Nov	EX (10:05)				E7 (14:30)				2
Dec	EX (10:30)				E7 (14:30)				2
Annual totals	6	3	3	0	3	9	4	1	29

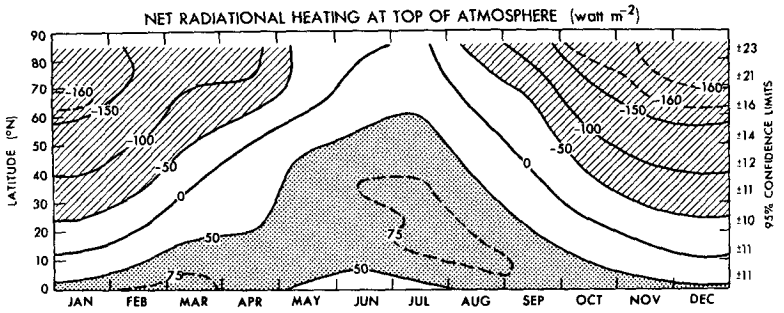

FIG. 2. Net incoming radiation flux at the top of the atmosphere (F_{TA}) based on satellite data as a function of latitude and month of the year. Annual mean 95% confidence limits are shown on the right hand side of the diagram (see Appendix for further information.) Units are in W m^{-2}.

and then averaged by level for 19 levels between the surface and 1000 m depth. In terms of 100 km by 100 km squares the Northern Hemisphere oceans (even in the tropics) are fairly well covered, with about 50% of the squares having at least one cast for each of the 12 calendar months. Interpolation for grid points with no data was carried out objectively through a Cressman (1959) type analysis scheme, using the annual mean temperature analyses as first guess fields. The main storage of oceanic energy was found to occur in the first 100 m. Nevertheless, since some measurable seasonal variation in temperature occurs below 100 m, it was decided after some experimentation to carry the vertical integration everywhere uniformly down to a depth of 250 m. The resulting values are thought to be probably the best oceanic heat storage estimates presently available. More information concerning the oceanic data set will be published in later papers.

4. Computations of the earth's heat budget

The external driving mechanism as well as the internal responses of the atmosphere and oceans are well known not only in a qualitative, but even in a semi-quantitative sense. Nevertheless, directly measured, reliable values of many of the seasonal heat balance components are not available in the literature. The most comprehensive study, as to overall depth and generality, probably still is the D.Sc. thesis at MIT of Gabites (1950). Some of the improvements in the data since 1950 are reflected in, e.g., the studies by Fritz (1958) and Newell *et al.* (1970, 1974). However, in the present paper, we attempt to exploit the significant advances in the basic data during the last 25 years for the first time to their full extent, to give "best" estimates of the large-scale heat balance components.

The different terms in the atmospheric and terrestrial branches of the energy cycle [Eqs. (7) and (8)] will be evaluated according to the logical sequence:

$$\underbrace{[F^{R}_{TA}+S_A+\mathrm{div}\mathbf{T}_A]}_{\text{atmospheric branch}} \rightarrow \underbrace{F_{BA}+[S_O+S_L+S_I]}_{\text{terrestrial branch}} \rightarrow \mathrm{div}\mathbf{T}_O$$

The results are presented both in graphical and tabular form as a function of latitude and month of the year. The graphs will make an easy appreciation of the most important features possible, while the tables are more useful for quantitative follow-up studies and comparisons by interested readers. All values given represent averages over entire 10° latitude belts containing, in general, both land and ocean points.

a. Atmospheric branch

For the present discussion, the balance equation (7) for the atmospheric branch of the earth's heat budget will be rewritten as follows:

$$\langle\bar{F}_{TA}\rangle=\langle\bar{S}_A\rangle+\langle\mathrm{div}\mathbf{T}_A\rangle+\langle\bar{F}_{BA}\rangle. \qquad (7a)$$

As before, brackets indicate spatial averages over 10° latitude wide belts and overbars temporal averages over 1 month.

The incoming solar radiation minus the sum of the reflected solar and emitted terrestrial radiation gives the net radiation flux (F_{TA}) at the top of the atmosphere. This driving component of the earth's general circulation is shown in Fig. 2. Annual mean 95% confidence limits (due to both natural variability and errors) are indicated on the right hand side of the diagram as a function of latitude. They were computed from the estimates of the standard error of the mean as given and discussed in the Appendix. These limits should give a rough idea of the reliability of the results. Fig. 2 shows in the tropics a broad heating band that roughly follows the annual declination curve of the sun. In middle and high latitudes, a strong cooling occurs in winter, and weak heating in summer. The actual monthly and annual values for 10° latitude belts and their hemispheric means are given in Table 2. In comparison with London's (1957) theoretical radiation estimates, the satellite measurements show extratropical differences of the order of 10 W m^{-2} or less for winter and summer. On the other hand, in spring the present values north of about 30°N tend to be 20 to 30 W m^{-2} lower, and in fall 10 to 20 W m^{-2} higher than

TABLE 2. Net radiational heating at the top of the atmosphere (W m^{-2}).*

North latitude	Jan	Feb	Mar	Apr	May	Jun	Jul	Aug	Sep	Oct	Nov	Dec	Annual
80–90°	−153	−148	−129	−107	−36	−3	1	−63	−126	−168	−159	−152	−104
70–80°	−157	−145	−102	−97	−39	11	18	−42	−95	−159	−161	−155	−94
60–70°	−156	−130	−78	−72	−12	42	48	−11	−50	−135	−158	−160	−73
50–60°	−144	−102	−56	−12	30	52	55	15	−18	−104	−138	−150	−48
40–50°	−114	−76	−23	20	57	68	65	37	−5	−65	−105	−122	−22
30–40°	−82	−46	7	34	68	78	79	57	11	−37	−76	−91	0
20–30°	−50	−13	35	42	66	68	76	61	37	−6	−42	−60	18
10–20°	−4	24	60	61	74	72	80	79	66	38	5	−13	45
0–10°	46	59	78	65	55	48	64	70	74	64	46	34	59
NH mean	−62	−32	10	23	49	59	66	46	19	−27	−57	−70	2

* 1 W m^{-2}=2.06 ly day^{-1}=0.0628 kcal cm^{-2} month^{-1}.

London's values. South of 20°N the new estimates are generally higher by 10 or 20 W m^{-2} throughout the year. Another point of interest is to consider the magnitude and phase of the annual and semiannual heating components which are presented in Table 11. Curiously enough, the semiannual component is not only important at low latitudes, as one would expect, but also at high latitudes. The annual and semiannual components together explain almost all the variance in the annual cycle. Also noteworthy is the general phase shift of the semiannual component between the tropics and polar regions from maxima around the middle of March and September to maxima around the beginning of January and July. The physical effects that cause these shifts require further study.

Part of the net incoming radiation will be used to increase the energy of the atmosphere through raising its temperature and simultaneously its specific humidity [Eq. (1b)]. The rate at which energy is stored (S_A) in the form of internal plus potential plus latent energy is given in Fig. 3. It shows that maximum storage occurs around May, maximum depletion during September and October, and that the maximum energy content is reached toward the end of July. However, it is also clear that in the overall heat balance the atmospheric storage plays only a minor role. The monthly and annual values for 10° latitude belts as well as the hemispheric means are given in Table 3, while the annual and semiannual contributions can be found in Table 11. As in the radiation case, the semiannual component is quite important both in high and low latitudes. It should be mentioned here that the values presented apply to the middle of the month, since they were computed from the difference in energy content between the following and the preceding months.

The divergence of the atmospheric flux of energy (div $\mathbf{T}_A$) is an important term in the atmospheric branch of the earth's heat budget. It is of the same magnitude as the incoming radiation flux. It contains the contributions due to not only fluxes of internal, potential and latent energy but also pressure work effects (for further information, see Oort, 1971). The net divergences by both mean and eddy fluxes are shown in Fig. 4. North of 60°N a belt of strong convergence of heat (mainly due to transient eddies) is in evidence throughout the year. A belt of general divergence of heat is found between 15 and 35°N. The pattern at middle latitudes is somewhat complicated, since the effects of mean meridional circulations and eddy circulations often counteract each other. The actual values of div $\mathbf{T}_A$ are given in Table 4, and further information concerning the annual and semiannual components in Table 11.

From the three heat balance components discussed above one can compute the energy flux (F_{BA}) between the atmosphere and the underlying earth's surface as

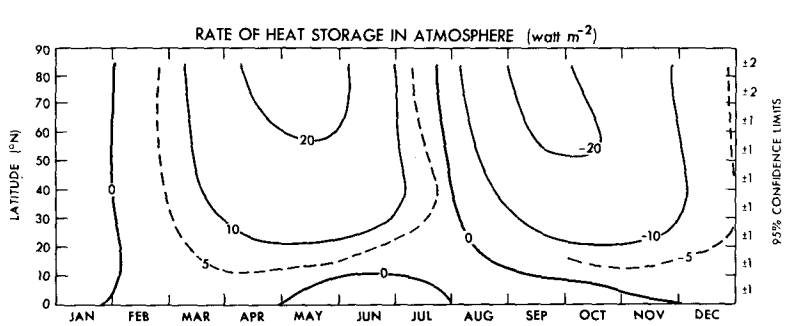

FIG. 3. Rate of heat storage in the atmosphere (S_A) based on radiosonde data as a function of latitude and month of the year. Units are in W m^{-2}.

TABLE 3. Rate of heat storage* in the atmosphere (W m^{-2}).

North latitude	Jan	Feb	Mar	Apr	May	Jun	Jul	Aug	Sep	Oct	Nov	Dec	Annual
80–90°	−2.2	2.3	11.2	20.3	24.0	19.1	2.8	−15.6	−23.1	−18.4	−12.8	−7.8	−0.0
70–80°	−2.2	2.3	11.2	20.3	24.0	19.1	2.8	−15.6	−23.1	−18.4	−12.8	−7.8	−0.0
60–70°	−0.7	2.6	10.1	19.2	22.1	18.7	4.3	−13.5	−21.8	−20.4	−14.0	−6.7	−0.0
50–60°	−1.1	3.4	10.3	16.8	19.0	17.3	5.9	−10.7	−19.7	−19.9	−14.4	−7.0	−0.0
40–50°	−2.5	3.1	10.3	15.7	17.7	17.0	7.8	−8.2	−18.5	−19.6	−14.7	−8.1	−0.0
30–40°	−2.8	2.3	8.2	13.5	16.5	16.1	7.8	−5.3	−15.2	−18.0	−14.5	−8.5	−0.0
20–30°	−2.3	2.3	6.5	10.7	12.5	9.0	3.4	−1.5	−8.6	−13.3	−11.5	−7.0	−0.0
10–20°	−2.2	1.1	4.4	6.6	5.0	1.6	0.9	0.6	−2.4	−5.5	−5.7	−4.4	−0.0
0–10°	−2.0	0.8	3.1	3.2	−0.8	−3.1	−0.6	0.9	1.0	0.3	0.8	−2.1	0.0
NH mean	−2.1	2.1	7.2	11.5	12.2	9.8	3.7	−4.7	−11.0	−12.6	−10.0	−6.1	−0.0

* Values for the 80–90°N belt were assumed to be equal to those for the 70–80°N belt.

a residual term in (7a). The results are shown in Fig. 5 and in Table 5. In general, there seems to be a substantial transfer of energy during the winter half year from the surface to the atmosphere with a maximum of more than 130 W m^{-2} at 50°N, and during the summer half year a transfer from the atmosphere into the surface of the order of 50 W m^{-2} or more at all latitudes. Traditionally, this exchange of energy has been computed from surface data only (e.g., Budyko, 1963). Thus radiation estimates and mean surface wind, temperature and humidity data were used in empirical formulas to derive the desired radiation, sensible heat and latent heat fluxes individually, as well as their sum, the net energy flux across the interface. Many uncertainties are involved both in the formulation and in the basic data used. On the other hand, the present estimates are directly computed from measured variables without any assumptions except that of conservation of energy. They should, therefore, be valuable as an independent check on the earlier results. For the months of January and July a detailed comparison was made with zonal averages based on Budyko's (1963) maps. The results are shown in Fig. 6. Budyko's January maps give fluxes ranging from −65 to −90 W m^{-2} between 20 and 60°N, where our fluxes tend to be stronger negative. South of 20°N our January fluxes are more positive, indicating a higher influx of energy into the oceans. In July north of 20°N there is fair overall agreement between the two methods, while south of 20°N our results are again substantially higher than Budyko's. This higher rate of transfer of radiational energy into the tropical oceans as derived from the more recent data has been discussed extensively by Vonder Haar and Suomi (1971) and Vonder Haar and Hanson (1969). The values of the annual and semiannual components are again tabulated in Table 11. They show a pattern roughly similar to that of the flux at the top of the atmosphere.

b. Terrestrial branch

For clarity of discussion the fundamental balance equation (8) for the terrestrial branch of the heat balance will be rewritten here in the form

$$\langle \bar{F}_{BA} \rangle = \langle \bar{S}_O \rangle + \langle \bar{S}_L \rangle + \langle \bar{S}_I \rangle + \langle \mathrm{div} \bar{\mathbf{T}}_O \rangle. \qquad (8a)$$

In words, the flux of energy from the atmosphere to the earth's surface in a certain belt can be used to heat the oceans and the land, and to melt snow and ice, while the remaining energy is transported away by the oceans. It may seem strange that the heat used in evaporation does not appear explicitly as a negative storage term

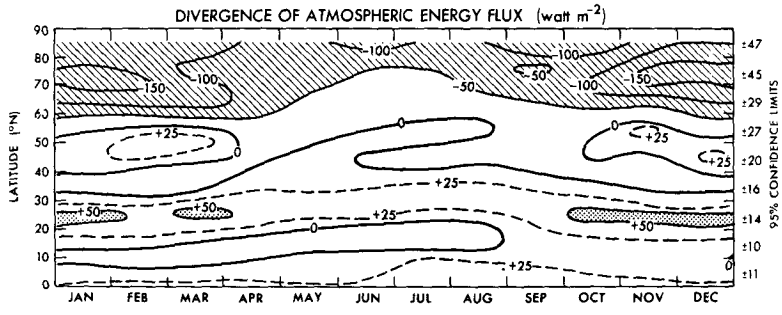

FIG. 4. Divergence of the energy transport due to atmospheric motions (div $\mathbf{T}_A$) based on radiosonde data as a function of latitude and month of the year. Units are in W m^{-2}.

TABLE 4. Divergence of atmospheric energy flux (W m^{-2}).

North latitude	Jan	Feb	Mar	Apr	May	Jun	Jul	Aug	Sep	Oct	Nov	Dec	Annual
80–90°	−100	−141	−118	−95	−90	−142	−89	−94	−191	−189	−143	−106	−125
70–80°	−160	−136	−87	−84	−95	−49	−43	−64	−45	−90	−155	159	−97
60–70°	−123	−135	−124	−92	−37	−20	−27	−26	−57	−88	−88	−106	−77
50–60°	−4	18	1	−15	−22	2	3	4	−13	−4	31	−31	−2
40–50°	19	32	6	−3	11	−2	−9	−10	−4	0	−3	26	5
30–40°	−16	−28	−17	23	18	25	28	34	23	2	−15	−20	5
20–30°	61	46	63	44	29	27	10	14	40	59	51	53	42
10–20°	4	3	−6	−4	−7	−13	−1	−4	10	14	14	18	2
0–10°	8	3	9	17	21	17	36	30	28	22	14	9	18
NH mean	−6	−8	−6	−1	1	3	6	5	6	2	−2	−6	−1

on the right-hand side of the equation. However, this effect is already included in the atmospheric branch and therefore appears as part of the term F_{BA} on the left-hand side of the equation. On the other hand, the heat of melting of snow and ice does appear as a possibly important term on the right-hand side. It should be mentioned that the sublimation process has not been properly taken into account because the latent heat of evaporation was used in all atmospheric calculations. In certain restricted situations the effects due to the difference in latent heat of evaporation (597 cal g^{-1}) and sublimation (677 cal g^{-1}) may be significant, but in general one may safely neglect these effects. Some other minor terms have also been left out of (8a) but they were discussed before in Section 2[1].

The oceans undoubtedly form the most important medium to store heat, at least on a seasonal time-scale. However, it is not obvious to what depth the annual cycle affects the oceanic temperature structure. In most areas of the globe the main influence is found in the first 100 m, but in isolated regions, such as the Norwegion Sea in winter, dense cold water may sink to much greater depths, and the annual cycle seems noticeable down to about 1000 m depth. The present authors have also investigated this problem based on the oceanic temperature analyses made at GFDL for 19 levels between the surface and 1000 m depth. Some month-to-month variations were found below 250 m, but they did not appear to be systematic or large enough to be trusted. Fig. 7 gives some idea of typical variations in the vertical. It shows the annual variation in hemispheric mean heat content of several oceanic layers between the surface and various depths. Based on this and similar evidence, the assumption was made that the heat content in the first 275 m of ocean represents everywhere the seasonally varying heat content.

[1] For example, the annual net transport of ice out of the Arctic Ocean has been estimated to be of the order of 3000 km^3 (Untersteiner, 1975, personal communication). This southward flow of ice would correspond to an effective northward flow of heat of about 0.008×10^{15} W, and can be neglected in comparison with the atmospheric and oceanic heat transports as given in Tables 9 and 10.

The rate of heat storage in this layer averaged over both ocean and land in 10° wide latitude belts is shown in Fig. 8 and tabulated together with the hemispheric mean in Table 6. For a breakdown into annual and semiannual components, see Table 11. The rate of heat storage reaches a maximum of more than 100 W m^{-2} at about 40°N in the middle of June and a minimum in the beginning of January. Most of this storage occurs east of North America over the Gulf Stream region and east of Asia over the Kuroshio, and is probably well correlated with the energy flux from the atmosphere F_{BA}. For more detailed information on the global distribution of the ocean heat storage one may refer to the excellent studies by Pattullo (1957), and Bryan and Schroeder (1960). The middle latitude pattern as shown in Fig. 8 agrees well both in magnitude and phase with that computed by Fritz (1958) based mainly on extrapolation of surface data [see also Newell *et al.* (1974, p. 31) for a summary of earlier studies]. However, south of 20°N Fritz' storage pattern is very flat (perhaps due to lack of data), while the present results show at 15°N a very distinct maximum in spring and a minimum in late summer. These features are mainly due to large systematic temperature changes in the eastern parts of the North Pacific and North Atlantic Oceans. Presumably upwelling and downwelling connected with changing surface wind patterns at these latitudes cause the apparent seasonal changes in local heat content of the oceans, since the energy flux from the atmosphere F_{BA} does not show a similar annual variation. As an independent check the present authors used grid point data of the hemispheric ocean temperature fields between the surface and 125 m depth (Bauer and Robinson, 1973) based on careful hand analyses by Mrs. Margaret K. Robinson to recompute the heat storage. At all latitudes the results were quite similar to those shown in Fig. 8, which reinforces the impression that the major features are well represented. Let us add as a final comment that typical oceanic values of the rate of heat storage can be obtained by dividing the gross averages shown in Table 6 by the percentage of ocean in each belt listed in the last column of the table. Because this percentage varies

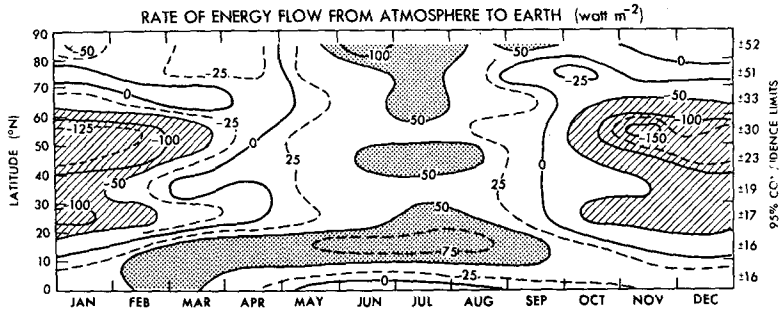

FIG. 5. Rate of energy flow from the atmosphere into the earth's surface (F_{BA}) computed as a residual term in the atmospheric branch of the heat balance as a function of latitude and month of the year. Units are in W m^{-2}.

with latitude and depth within the 10° belt, it is not possible to exactly reconstruct typical oceanic values. However, the differences are small. Maximum typical storage values are found between 30 and 50°N and reach almost 200 W m^{-2}.

The rate at which heat is stored in land S_L has been estimated by Gabites (1950). It was found to be very small compared with the oceanic storage. For example, his values reach a minimum of -5 W m^{-2} in December and a maximum of 5 W m^{-2} in July, both located in the 60–70°N belt where almost 75% of the belt is taken up by land. Thus it appears justified to neglect the heat storage in land in (8a) in further calculations.

Estimates of the storage of energy due to melting of snow and ice and the negative storage involved in ice formation, which are both contained in the term S_I in (8a), are not readily available in the literature. Relevant information on certain aspects of the problem may be found in, for example, a study by Maykut and Untersteiner (1971) on sea ice, and in Kukla and Kukla's (1974) or Wiesnet and Matson's (1975) monthly estimates of the total area covered by snow and ice. However, these papers do not supply the quantitative information needed for the present study. Therefore, the results of a numerical model of the joint ocean-atmosphere system by Wetherald and Manabe (1972) were used as an additional guide to derive order of magnitude estimates. One useful result is the model snow depth as a function of latitude and month of the year which these authors computed for an idealized land-sea configuration (see their Fig. 11). Based on the sources mentioned above and on estimates of ice growth and ice melt in the Arctic by Untersteiner (1975, personal communication) the authors have made an extremely crude evaluation of the rate of heat storage in snow, sea ice and ground ice for the different seasons. These estimates are shown in Table 7. In the Arctic north of 70°N, significant melting (positive heat storage) occurs only during the summer months. The arctic snow and ice pack seems to grow (negative heat storage) during the rest of the year. South of 70°N most of the snow and ice melts in spring and early summer, whereas snow accumulation and ice formation take place in fall and winter. Because of the tentative nature of our estimates of $\langle \bar{S}_I \rangle$ they were not used in the later residual calculations. Thus the flux divergence of heat by oceanic motions $\langle \text{div } \overline{\mathbf{T}}_O \rangle$ and the heat transport by oceanic motions $\langle \overline{\mathbf{T}}_O \rangle$ were computed assuming $\langle \bar{S}_I \rangle = 0$ in order to avoid a possible bias in the results. In any case, if the values of $\langle \bar{S}_I \rangle$ in Table 7 had been used the corrections to Tables 8 and 10 would have been small, except possibly in the Arctic. The primary purpose in presenting Table 7 is to show

TABLE 5. Rate of energy flow from atmosphere to earth (W m^{-2}).

North latitude	Jan	Feb	Mar	Apr	May	Jun	Jul	Aug	Sep	Oct	Nov	Dec	Annual
80–90°	−52	−10	−23	−32	30	119	88	47	89	39	−2	−38	21
70–80°	5	−11	−26	−34	32	41	59	37	−27	−50	8	12	4
60–70°	−32	2	36	0	4	43	72	28	28	−26	−56	−48	4
50–60°	−138	−123	−67	−14	32	33	46	21	14	−80	−154	−112	−45
40–50°	−130	−110	−40	8	29	53	66	56	18	−46	−87	−140	−27
30–40°	−64	−21	16	−3	34	37	43	28	4	−21	−46	−63	−5
20–30°	−109	−61	−35	−12	24	32	62	48	5	−52	−81	−106	−24
10–20°	−6	20	62	58	75	83	81	82	57	30	−3	−26	43
0–10°	40	56	66	45	35	34	29	38	45	42	33	27	41
NH mean	−53	−26	8	13	36	47	57	46	24	−16	−44	−57	3

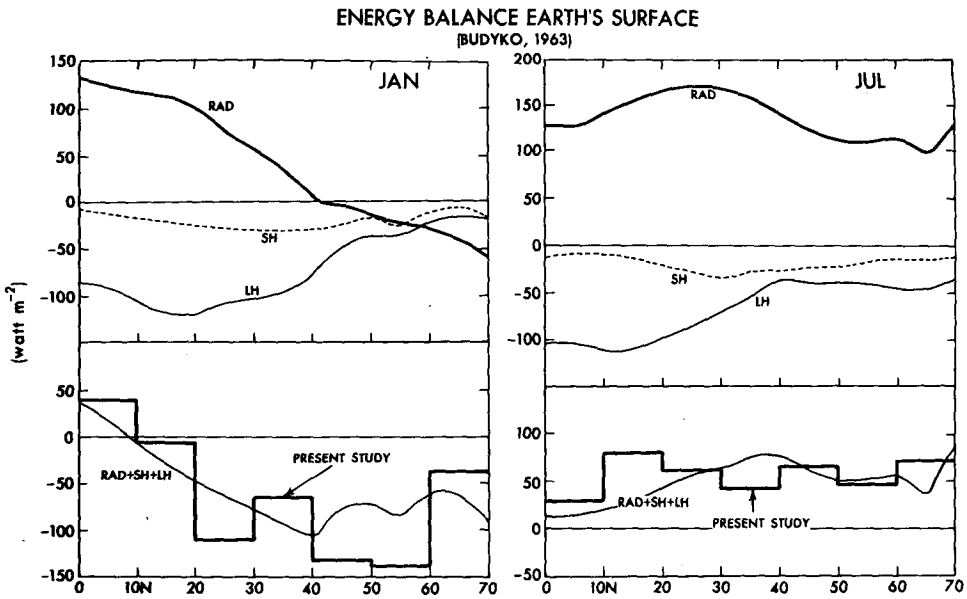

FIG. 6. Comparison of the energy balance components (RAD, SH and LH) at the earth's surface according to Budyko (1963) with the net rate of energy flow F_{BA} as computed in the present study. Units are in W m^{-2}.

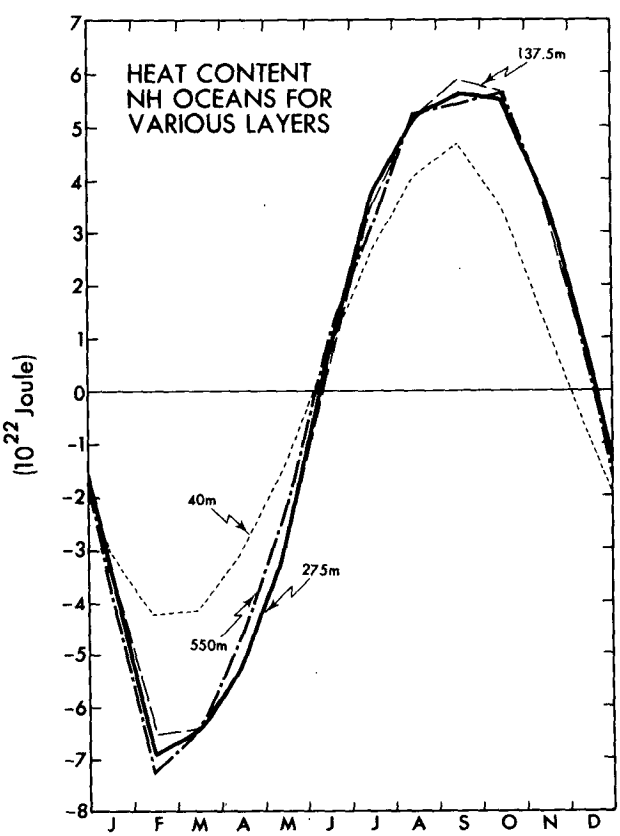

FIG. 7. Oceanic heat content of various hemispheric layers between the surface and 40, 137.5, 275 and 550 m depth as a function of month of the year. Units are in 10^{22} J for the hemisphere (multiply numbers by 0.391 and 0.640 to find average heat content per unit "land and ocean" and "ocean only" areas, respectively, in units of 10^8 J m^{-2}).

the urgent need for better estimates of the storage of energy in the cryosphere in view of our meager present knowledge.

The final term to be discussed is the rate at which oceans motions transport energy into or out of the different latitude belts (div $\mathbf{T}_O$). As remarked earlier it seems almost hopeless to attempt to measure this transport directly from ocean current data. Instead the oceanic heat convergence is computed indirectly as a residual in (8a). The storage terms in land, snow and ice are neglected but this would probably introduce an error of at most 10 W m^{-2} (except in the Arctic during summer), which is probably smaller than the uncertainty in the remaining terms F_{BA} and S_O. The computed divergence pattern is shown in Fig. 9, while the actual values averaged over entire 10° latitude wide belts are given in Table 8. Typical oceanic values can again be obtained by dividing the numbers by the percentage area covered by oceans in each belt. It is evident from Fig. 9 that the oceanic motions play a crucial role in the terrestrial heat budget, and that their effects are comparable in magnitude to those of the influx from the atmosphere and the rate of heat storage in the oceans. A major feature of interest seems to be the strong convergence of heat between 45 and 60°N in winter. One may speculate that this convergence mainly takes place in the western parts of the oceans where dry and cold continental air flows out over the warm oceans, and extracts large amounts of heat from the oceans. However, in early summer the convergence region apparently decreases somewhat in intensity and moves southward to the 30–40°N belt. Divergence of heat is generally found south of 20°N, with a very

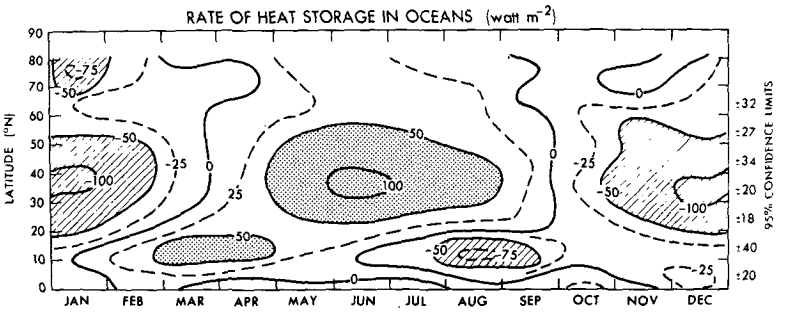

FIG. 8. Rate of heat storage in the oceans (S_O) based on hydrographic stations, MBT and XBT data as a function of latitude and month of the year. Units are in W m^{-2}. To obtain typical oceanic values divide by the percentage of the horizontal area covered by oceans (factor=0.61 for the Northern Hemisphere as a whole).

pronounced maximum in summer of about 150 W m^{-2}. In Subsection 4d, it will be shown that this feature implies a strong southward flow of heat across the equator during the northern summer. The breakdown of the divergence field into annual and semiannual components is shown in Table 11.

An unrealistic feature in our analysis of $\langle \text{div } \overline{\mathbf{T}}_O \rangle$ seems to be the positive divergence computed at arctic latitudes. Especially during the winter and summer seasons this would necessitate a substantial southward transport of heat out of the Arctic Ocean. However, such an export of heat seems to contradict the available direct evidence presented by Aagaard and Greisman (1975).

c. *The overall heat balance*

To summarize the information discussed above, some figures have been prepared that may bring out more clearly which terms dominate the heat balance in the different latitude belts. Thus Fig. 10 shows the latitudinal profiles for the cooling (September through February) and heating (March through August) semesters. The semesters are chosen in such a way that the rate of total heat storage in atmosphere plus oceans is a maximum in the heating semester.

North of 60°N in both semesters the main balance seems to be between radiative cooling and the convergence of energy by atmospheric motions. South of 20°N radiative heating is found to be balanced primarily by the divergence of heat by oceanic motions. Between 20 and 60°N the situation is more complex. In the cooling semester the radiative heat loss at the top of the atmosphere is balanced by a cooling of both the atmosphere and the oceans plus a convergence of heat by oceanic motions. Around 25°N there seems to be, in addition to the radiative heat loss, an important cooling due to atmospheric motions. In the heating semester about half of the net incoming radiational energy between 20 and 60°N is apparently used either to locally heat the atmosphere or to export heat toward high latitudes, while the remaining half is stored in the oceans. In fact, the storage in the oceans at these latitudes is so large according to our analyses that it requires in addition a strong convergence of heat due to oceanic motions.

In Fig. 11, different panels show the heat balance components averaged over the entire Northern Hemi-

TABLE 6. Rate of heat storage in oceans (W m^{-2}).*

North latitude	Jan	Feb	Mar	Apr	May	Jun	Jul	Aug	Sep	Oct	Nov	Dec	Annual	Percent ocean
80–90°	(−59)**	(−28)	(49)	(20)	(27)	(20)	(30)	(7)	(−18)	(−28)	(−30)	(10)	−0	89.9
70–80°	−78	−31	−9	−10	38	40	28	23	5	−5	16	−17	0	67.3
60–70°	−23	−5	−11	4	19	28	30	27	−6	−23	−9	−31	0	26.3
50–60°	−49	−43	−6	18	50	59	50	36	17	−27	−61	−44	0	41.9
40–50°	−96	−70	−10	28	71	80	67	58	28	−20	−61	−77	0	49.5
30–40°	−102	−68	−16	28	88	115	91	71	23	−38	−86	−107	0	58.2
20–30°	−83	−34	10	35	54	56	41	38	24	−9	−46	−85	−0	63.0
10–20°	−22	26	66	64	36	21	−24	−75	−50	−18	−6	−18	0	74.3
0–10°	−14	16	26	10	4	12	11	−16	−5	12	−22	−34	−0	78.2
NH mean	−56	−23	12	27	45	50	34	14	3	−15	−38	−54	−0	61.0

* Values represent the rate at which heat is stored in each 10° latitude belt divided by the area of the entire belt containing both ocean and land points in general. To obtain approximate values representative of oceans only, or in other words, typical oceanic values, divide values by the percentage area covered by oceans given in the last column.

** Since only very few seasonal data were available north of 80°N, the results for the 80–90°N belt are unreliable.

TABLE 7. Tentative "order-of-magnitude" estimates of the rate of heat storage* in snow, sea ice and ground ice (W m^{-2}) for the four seasons (DJF = December, January and February, etc.).

North latitude	DJF	MAM	JJA	SON	Annual
80–90°	−5	−5	20	−10	0
70–80°	−5	−3	16	−8	0
60–70°	−5	3	5	−3	0
50–60°	−2	4	0	−2	0
40–50°	−2	2	0	0	0
0–40°	0	0	0	0	0
NH mean	−1.1	0.7	1.4	−0.9	0.0

* Melting of 10 cm (water equivalent) snow or ice in one month requires 12.7 W m^{-2}.

sphere, the tropics, and middle and high latitudes. For the hemisphere as a whole, the present analysis suggests that the primary balance is between radiational influx, oceanic heat storage, and cross-equatorial flow of heat in the oceans. However, atmospheric storage, which reaches its maximum 1.5 months before the oceanic storage, is by no means negligible. In the tropics, except for mid-winter, the excess radiation flux is found to be balanced by oceanic heat storage during the first semester and by the divergence of heat in the oceans during the second semester. There is also a steady but smaller removal of heat due to atmospheric motions. North of 30°N we find very large summer-winter differences, especially in the radiation influx and in the atmospheric and oceanic storage values. Throughout the year the atmosphere and oceans transport energy into this region.

d. Atmospheric and oceanic heat fluxes

In the atmosphere the transfer of sensible heat, potential energy and latent heat all give important contributions, and have been included in the calculation of div $\mathbf{T}_A$ [Eq. (1g)]. The transfer mechanism at low latitudes is through mean meridional circulations and at middle and high latitudes predominantly through show the net atmospheric transports calculated directly from observations. Maximum poleward fluxes of the order of 5×10^{15} W are found in winter in middle latitudes, decreasing to about 1.5×10^{15} W in summer. Near the equator there is an interesting seasonal reversal in the meridional circulation that causes the transport to be in general from the summer to the winter hemisphere. Further details can be found in Oort (1971). The amplitude and phase of the annual and semiannual components are presented in Table 12.

In the oceans the expression (1h) for the transport of energy may be simplified considerably because contributions by the pressure work term and the transport of potential energy almost completely compensate each other. In fact, in an ocean of uniform density one can show that these terms cancel each other exactly (Jung, 1952). Thus only the transport of internal energy has to be considered. In spite of this simplification it is not feasible to compute the oceanic energy flux directly from observations as we have argued before. Thus at present, one of the only practical methods seems to be through indirect means such as the residual method discussed in Subsection 4b. There are of course also difficulties involved in the residual method. For example, quasi-horizontal eddy circulations. Fig. 12 and Table 9 the uncertainties in each individual component will affect the final residual. This problem is considered further in the Appendix. Through integration of div $\mathbf{T}_O$ in Table 8 southward from the North Pole over progressively larger polar caps estimates of $\mathbf{T}_O$, the vertically integrated oceanic heat transport, were obtained as a function of latitude. The resulting values are shown in Fig. 13 and tabulated in Table 10. The oceanic transports are found to be of major importance south of 40°N where the atmospheric transports tend to be weaker. The strongest northward fluxes by the ocean are of the order of 5×10^{15} W and are found to occur between 10 and 20°N in spring and fall, and not in winter as in the atmosphere. In winter the computed transports are not only weaker but also tend to occur at higher latitudes (about 40°N). North of 60°N the

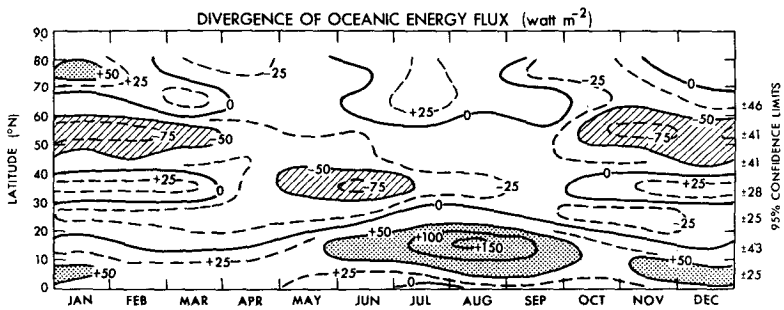

FIG. 9. Divergence of the energy transport due to oceanic motions (div $\mathbf{T}_O$) computed as a residual term in the terrestrial branch of the heat balance as a function of latitude and month of the year. Units are in W m^{-2}. To obtain typical oceanic values divide by the percentage of the horizontal area covered by oceans.

TABLE 8. Divergence of oceanic energy flux (W m^{-2}).*

North latitude	Jan	Feb	Mar	Apr	May	Jun	Jul	Aug	Sep	Oct	Nov	Dec	Annual
80–90°	(7)	(19)	(−72)	(−52)	(3)	(100)	(57)	(40)	(106)	(67)	(28)	(−48)	(21)
70–80°	83	20	−17	−24	−6	1	31	14	−32	−45	−8	29	4
60–70°	−9	8	47	−3	−16	14	42	1	34	−4	−47	−17	4
50–60°	−89	−80	−62	−32	−18	−26	−4	−15	−2	−53	−92	−68	−45
40–50°	−34	−41	−30	−21	−42	−27	−1	−2	−11	−26	−27	−63	−27
30–40°	38	47	32	−31	−55	−78	−48	−42	−20	17	39	44	−5
20–30°	−26	−27	−45	−47	−30	−24	22	10	−19	−43	−35	−20	−24
10–20°	16	7	−4	−6	39	63	105	158	107	47	2	−8	43
0–10°	54	40	40	35	31	21	18	54	50	30	55	61	41
NH mean	4	−3	−5	−15	−9	−4	22	31	22	−1	−6	−3	3

* Values represent the rate at which oceanic motions transport heat out of each 10° latitude belt divided by the total area in the belt. To obtain approximate values representative of the oceans only, i.e., typical oceanic values, divide by the percentage area covered by oceans given in the last column of Table 6.

oceanic transports are quite weak and seem to be predominantly toward the south, in disagreement with available direct evidence (Aagaard and Greisman, 1975). In equatorial latitudes cross-equatorial transports are found to be generally of the same sign but much stronger than the atmospheric transports. In fact, the strongest heat flux of -8.1×10^{15} W is computed to occur at the equator in August. Thus in general, both atmosphere and oceans seem to transport heat from the summer into the winter hemisphere. It should

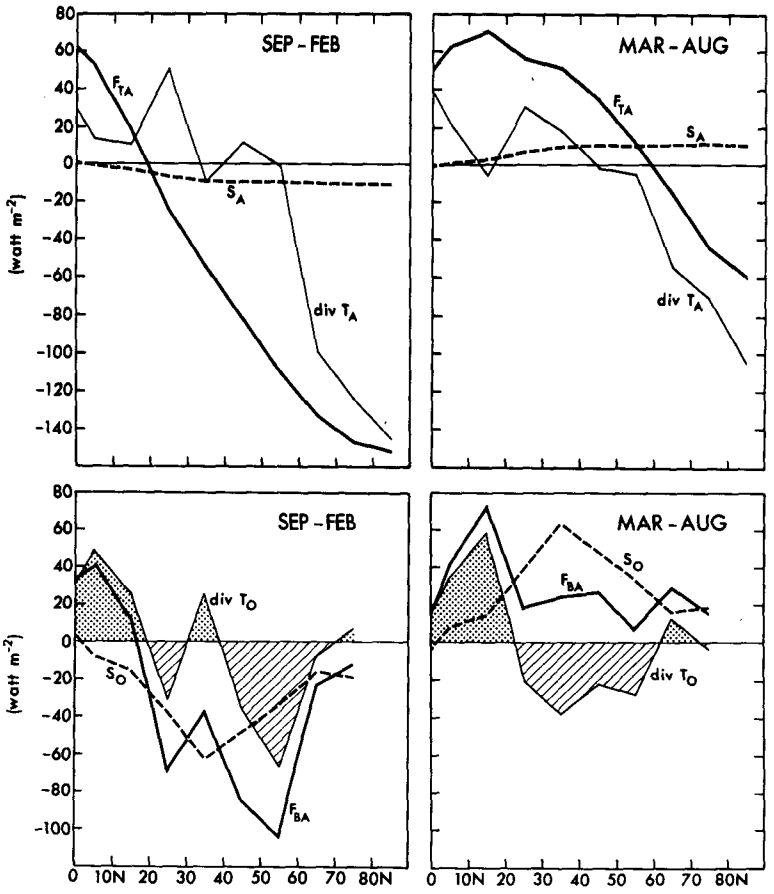

FIG. 10. Latitudinal distribution of various components in the atmospheric (top) and terrestrial (bottom) branches of the earth's heat balance for the cooling (September through February) and heating (March through August) semesters. Units are in W m^{-2}.

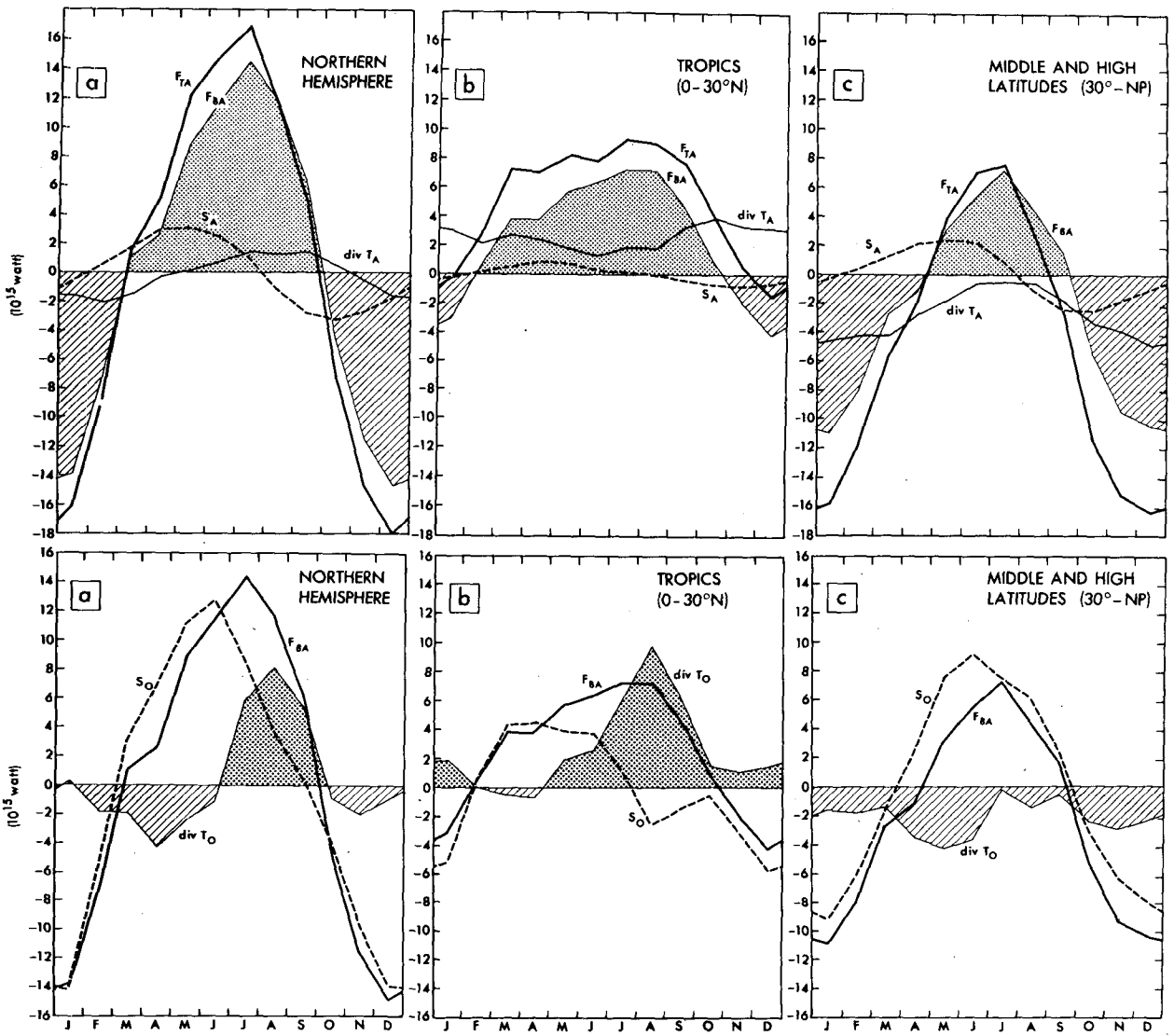

FIG. 11. Annual variation of various components in the atmospheric and terrestrial branches of the heat balance integrated over (a) the Northern Hemisphere, (b) tropics, and (c) middle and high latitudes. Units are in 10^{15} W (multiply numbers by 3.91, 7.81 and 7.81, respectively, to find average values per unit "land and ocean" area in W m^{-2}).

perhaps be mentioned again that the uncertainty in these residual calculations of ocean transport must be quite large as suggested by the 95% confidence limits given in Fig. 13. A breakdown of the oceanic heat transports in their annual and semiannual components is given in Table 12.

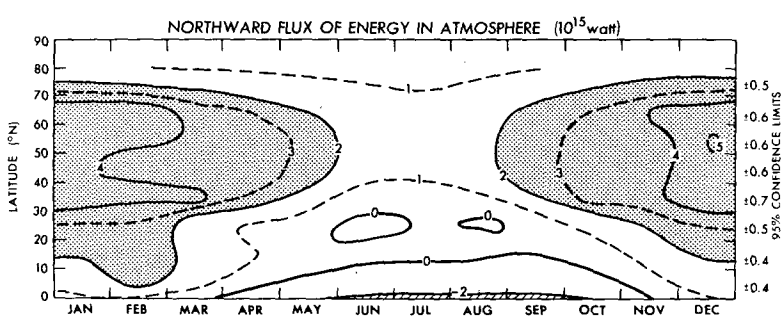

FIG. 12. Northward transport of energy due to atmospheric motions (T_A) based on radiosonde data. Units are in 10^{15} W.

TABLE 9. Northward flux of energy in the atmosphere (10^{15} W).*

North latitude	Jan	Feb	Mar	Apr	May	Jun	Jul	Aug	Sep	Oct	Nov	Dec	Annual
80°	0.4	0.5	0.5	0.4	0.3	0.6	0.3	0.4	0.7	0.7	0.6	0.4	0.5
70°	2.2	2.1	1.5	1.3	1.4	1.1	0.8	1.1	1.3	1.8	2.4	2.3	1.6
60°	4.6	4.7	3.8	3.1	2.1	1.5	1.4	1.6	2.3	3.4	4.0	4.3	3.1
50°	4.7	4.2	3.8	3.5	2.7	1.4	1.3	1.5	2.7	3.5	3.2	5.0	3.1
40°	4.1	3.2	3.6	3.6	2.4	1.5	1.6	1.8	2.8	3.5	3.3	4.2	3.0
30°	4.6	4.2	4.2	2.7	1.7	0.6	0.5	0.6	1.9	3.4	3.9	4.9	2.8
20°	2.2	2.4	1.6	0.9	0.5	−0.5	0.1	−0.0	0.3	1.1	1.8	2.8	1.1
10°	2.0	2.2	1.9	1.1	0.8	0.1	0.2	0.2	−0.1	0.4	1.2	2.1	1.0
0°	1.6	2.1	1.5	0.3	−0.1	−0.7	−1.4	−1.2	−1.4	−0.5	0.6	1.7	0.2

* 10^{15} W $=0.754\times10^{22}$ cal year$^{-1}=6.29\times10^{20}$ cal month^{-1}.

For comparison, some annual mean estimates from earlier studies are given in the last two columns of Table 10. The first of the previous studies was made some years ago by the present authors only for the annual case (Vonder Haar and Oort, 1973) using the same technique but slightly different satellite radiation data. The differences in final results are small, except south of 20°N where the present estimates of ocean transport tend to be less positive. The second comparison is with Budyko's estimates based on surface climatological data as summarized by Sellers (1965). His values are about a factor of 2 smaller than the present ones, but also show a low latitude maximum. As was mentioned before, these surface estimates are questionable mainly because of the assumptions made in the flux-gradient relationships.

Many different scales of motion could contribute to the oceanic transports, and add to the difficulty of direct measurements. For example, one can think of slow (but quite efficient) meridional overturnings, Ekman drifts, intense western boundary currents, mesoscale and even large-scale eddies. At specific locations and for short periods many excellent studies have been made of the transports based on direct oceanic observations. The reader may refer, e.g., to Bryan (1962) for some sections in the Atlantic and Pacific Oceans, Wyrtki (1965) for the equatorial Pacific Ocean, Niiler and Richardson (1973) for the Florida Current, and Aagaard and Greisman (1975) for the Arctic Ocean. Nevertheless, no direct, zonally averaged estimates seem to be available in the literature for a meaningful comparison with the present results.

5. Summary and concluding remarks

In the present study the annual cycle in the heat balance of the earth, comprised of the atmosphere, oceans, land and cryosphere, is investigated in detail over the Northern Hemisphere.

A unique feature is that available satellite radiation, atmospheric and oceanic data have been brought together to make quantitative estimates of all major components of the heat budget. The results reported here are based completely on observations with no assumptions other than that of the representiveness of the data samples used. In short, the three basic samples are (1) a data set of reflected solar and infrared terrestrial radiation measurements for earth orbiting satellites for the period 1964–1971, (2) a 5-year data set of daily atmospheric observations from about 600 radiosonde stations over the Northern Hemisphere for the period 1958–1963, and (3) a long-term data set of all oceanographic temperature observations in the NODC files of hydrographic station, MBT and XBT data.

In the present formulation the earth's heat balance is broken down into an atmospheric and a terrestrial branch in analogy with the usage in hydrology. The atmospheric branch includes the net incoming flux of

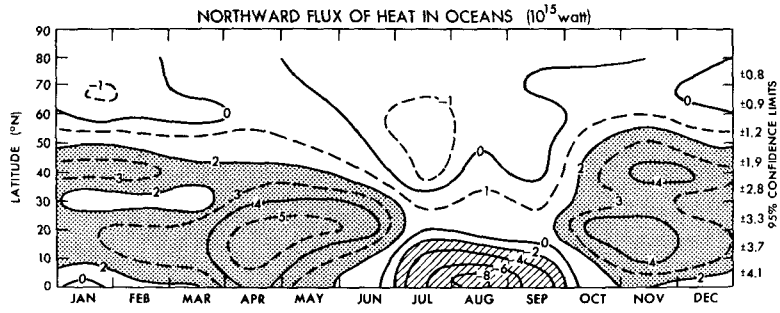

FIG. 13. Northward transport of heat due to oceanic motions (T_O) computed as a residual term in the earth's heat balance. Units are in 10^{15} W.

TABLE 10. Northward flux of heat in oceans (10^{15} W).

North latitude	Jan	Feb	Mar	Apr	May	Jun	Jul	Aug	Sept	Oct	Nov	Dec	Annual	(1)	(2)
80°	0.0	−0.1	0.3	0.2	0.0	−0.4	−0.2	−0.2	−0.4	−0.3	−0.1	0.2	−0.1	−0.1	0.0
70°	−1.0	−0.3	0.5	0.5	0.1	−0.4	−0.6	−0.3	−0.0	0.3	−0.0	−0.1	−0.1	0.1	0.1
60°	−0.8	−0.4	−0.4	0.5	0.4	−0.7	−1.4	−0.3	−0.7	0.3	0.9	0.2	−0.2	0.1	0.3
50°	1.5	1.6	1.2	1.4	0.8	−0.0	−1.3	0.0	−0.6	1.7	3.2	1.9	1.0	1.1	0.8
40°	2.5	2.9	2.1	2.0	2.2	0.8	−1.2	0.1	−0.3	2.5	4.1	3.9	1.8	2.1	1.0
30°	1.1	1.2	0.9	3.2	4.2	3.7	0.5	1.7	0.4	1.9	2.7	2.3	2.0	2.5	1.5
20°	2.2	2.3	2.8	5.1	5.4	4.7	−0.3	1.2	1.2	3.7	4.1	3.1	2.9	3.4	1.6
10°	1.5.	2.6	2.9	5.3	3.7	2.0	−4.9	−5.6	−3.4	1.6	4.0	3.5	1.1	1.9	1.1
0°	−0.9	0.8	1.2	3.8	2.3	1.0	−5.7	−8.0	−5.6	0.3	1.5	0.7	−0.7	0.3	−0.2

(1) Previous annual mean estimate by Vonder Haar and Oort (1973) using same technique as used here, but slightly different data.
(2) Annual mean estimate based on Budyko's (1963) surface climatological data as compiled by Sellers (1965).

radiation at the top of the atmosphere, the storage of energy in the atmosphere, the divergence of energy due to atmospheric transports, and finally the flux of energy into the earth's surface. This last component was computed as a residual in the atmospheric branch. It forms the link with the terrestrial branch, which contains as additional terms the storage of energy in the oceans, the land and the cryosphere as well as the divergence of energy due to oceanic transports. The oceanic divergence was computed as a residual in the terrestrial branch of the heat budget.

The results for the heat balance components were presented both in graphical and tabular form as averages for 10° wide latitude belts and for the 12 calendar months. Order of magnitude estimates for the storage of energy in land and in snow and ice indicate that in general these terms are small in comparison with the storage in atmosphere and oceans, and that

TABLE 11. Amplitude (W m^{-2}), phase of first maximum (number of months following 1 January) and variance (%) explained by the annual plus semiannual components for various heat balance terms.

North latitude	F_{TA}*					S_A					div T_A				
	C_1	ϕ_1	C_2	ϕ_2	%	C_1	ϕ_1	C_2	ϕ_2	%	C_1	ϕ_1	C_2	ϕ_2	%
80–90°	77	5.7	32	0.0	99	20.6	3.7	6.9	5.0	100	27	3.6	23	0.1	51
70–80°	85	5.8	26	0.3	98	20.6	3.7	6.9	5.0	100	55	6.3	20	2.3	92
60–70°	101	5.8	20	0.6	98	20.0	3.7	6.3	5.2	100	54	6.7	14	5.4	98
50–60°	104	5.7	8	1.4	99	18.7	3.8	4.9	5.4	100	4	10.3	5	1.5	8
40–50°	98	5.7	6	2.4	100	18.2	3.9	4.3	5.5	100	15	1.0	5	0.3	72
30–40°	87	5.6	7	2.2	100	16.5	4.1	3.7	5.7	100	29	6.4	2	3.3	89
20–30°	66	5.7	14	2.4	99	11.8	4.1	1.2	0.0	99	20	0.3	9	3.4	86
10–20°	43	5.8	15	2.5	99	5.3	4.1	1.2	2.5	97	12	10.6	2	4.0	89
0–10°	7	5.9	16	2.4	94	0.7	3.3	2.4	2.7	87	13	7.1	2	2.1	89
NH mean	66	5.7	9	2.0	99	12.0	3.9	1.9	5.3	100	7	7.1	1	9.2	98
North latitude	F_{BA}					S_O					div T_O				
	C_1	ϕ_1	C_2	ϕ_2	%	C_1	ϕ_1	C_2	ϕ_2	%	C_1	ϕ_1	C_2	ϕ_2	%
80–90°	68	6.9	7	0.4	80	31	4.9	6	3.9	54	60	7.8	12	0.6	61
70–80°	23	6.1	37	0.0	87	37	6.5	16	4.4	78	15	1.0	41	0.4	88
60–70°	43	5.6	25	1.5	89	27	5.8	6	0.4	90	16	5.3	23	1.8	60
50–60°	98	6.0	6	2.0	94	58	5.7	2	0.5	97	41	6.3	7	2.3	87
40–50°	101	6.1	14	2.7	99	86	6.0	10	3.6	99	17	7.0	11	2.0	73
30–40°	50	5.7	10	2.1	94	109	5.8	0	5.1	100	59	0.0	10	2.1	96
20–30°	78	6.0	13	1.8	98	66	5.7	19	3.1	99	17	7.3	20	0.7	88
10–20°	50	5.7	14	2.3	98	50	2.9	25	3.9	92	67	7.3	29	1.4	95
0–10°	8	2.1	12	2.4	89	16	4.2	11	2.6	60	14	11.2	2	1.5	54
NH mean	54	5.9	10	2.0	99	50	5.4	9	3.4	99	14	8.0	13	1.3	94

* C_1, C_2 = amplitudes of annual and semiannual components.
ϕ_1, ϕ_2 = phases of annual and semiannual components.
% = percentage of total variance explained by annual plus semiannual components.

TABLE 12. Amplitude (10^{15} W), phase of first maximum (number of months following 1 January) and variance (%) explained by the annual plus semiannual components of the atmospheric and oceanic heat fluxes.

North latitude	T_A C_1	ϕ_1	C_2	ϕ_2	%	T_O C_1	ϕ_1	C_2	ϕ_2	%
80°	0.1	9.6	0.1	3.1	51	0.2	1.8	0.0	3.6	61
70°	0.7	0.0	0.2	5.0	94	0.1	3.3	0.5	3.4	84
60°	1.7	0.4	0.1	3.0	99	0.3	0.0	0.7	4.0	77
50°	1.6	0.5	0.2	3.7	92	1.3	0.3	0.8	4.2	84
40°	1.2	0.3	0.3	3.5	90	1.8	0.5	1.1	4.5	91
30°	2.2	0.4	0.3	3.6	98	0.6	4.3	1.3	4.6	79
20°	1.4	0.4	0.1	0.0	95	0.9	2.7	1.9	4.3	84
10°	1.1	1.1	0.2	0.5	96	3.6	1.6	3.2	4.3	96
0°	1.7	1.1	0.2	0.2	98	3.5	2.0	3.3	4.3	94

they may therefore be neglected. Generalizing, the computations show that at high latitudes the primary balance occurs between the net outflow of radiation at the top of the atmosphere and the convergence of heat due to atmospheric motions. In the tropics the net inflow of radiation was found to be balanced mainly by the divergence of heat due to oceanic motions. Finally, in middle latitudes the situation is more complex and all terms, atmospheric and oceanic storage as well as flux divergence, seem to be important in the energy balance. Many other features of interest regarding annual cycles were noticed in the distributions of the different components, but these discussions will not be repeated here. It should be mentioned though that the present method supplies for the first time fairly reliable, quantitative estimates of the seasonal cycle in the oceanic transports of heat. Compared to the atmospheric transports the oceanic transports appear to dominate in the tropics. The oceans are found to transport large amounts of heat across the equator, generally in the direction of the winter hemisphere. In the Appendix the possible errors involved in the different estimates are presented and discussed.

From the evidence presented above it seems obvious that the oceans play a crucial role in determining the climate on earth. One of the major tasks for the near future will be to obtain representative measurements of the oceanic transports *in situ* through large-scale international observational programs. It is hoped that the present paper will help focus such efforts. In addition, numerical models of the ocean circulations will hopefully improve to the point that realistic transport values will be computed, and that thereby the role of different scales of motion will be shown.

Although the storage of energy in snow and ice was found to be small compared to the other terms in the earth's heat balance, this does not mean that snow and ice do not play an important role in the climate. For example, it is well-known that snow and ice practically dominate the radiation balance at high latitudes because of their high albedo. Our only contention is that the annual variation in the heat stored in snow and ice is relatively small. However, on a longer time-scale of the order of hundreds or thousands of years this storage may become very significant, perhaps even larger than the oceanic storage.

Acknowledgments. The authors thank Jim Ellis of Colorado State University and Sydney Levitus of the Geophysical Fluid Dynamics Laboratory (GFDL) for their invaluable assistance in the analysis of the basic radiation and oceanographic data, respectively, and are grateful to Betty Williams, Mel Rosenstein, Hilda Philander, John Conner, and Phil Tunison and his co-workers at GFDL for various help in the preparation of the manuscript. The authors are also indebted to Norbert Untersteiner for information on arctic ice conditions, and to Syukuro Manabe, Kirk Bryan, and the official reviewers for useful comments on the manuscript. Finally, the first author would like to express his gratitude to Joseph Smagorinsky for his generous support of this work.

APPENDIX A

List of Symbols

C_A, C_I, C_L, C_O	specific heat at constant volume for atmosphere, snow and ice, land, ocean
div	horizontal divergence operator
E	total energy
F_{BA}, F_{TA}	local vertical flux of energy at bottom, top of atmosphere
g	acceleration due to gravity
L_e, L_m	latent heat of evaporation, melting
p	pressure
q	specific humidity of air
S_A, S_I, S_L, S_O	rate of storage of energy in atmosphere, snow and ice, land, ocean
t	time
T	temperature
$\mathbf{T}_A$, $\mathbf{T}_O$	horizontal transport of energy in atmosphere, ocean
$\mathbf{V}$	horizontal velocity vector
Z	height
∇_2	horizontal divergence operator
ρ	density

TABLE 13. Standard error of the mean (W m^{-2}) for various terms in the heat balance for typical winter, spring, summer and fall months.

North latitude	$\sigma(F_{TA})/\sqrt{N}$*				$\sigma(\text{div } \mathbf{T}_A)/\sqrt{N}$				$\sigma(F_{BA})/\sqrt{N}$**				$\sigma(S_O)/\sqrt{N}$			
	DJF	MAM	JJA	SON	DJF	MAM	JJA	SON	DJF	MAM	JJA	SON	DJF	MAM	JJA	SON
80–90°	14	5	11	13	29	25	12	25	32	25	17	28	—	—	—	—
70–80°	14	7	13	13	33	15	8	26	36	17	15	29	—	—	—	—
60–70°	7	9	11	4	20	16	9	11	21	18	14	12	12	10	17	22
50–60°	2	9	9	5	19	11	11	11	19	14	14	12	18	10	12	12
40–50°	7	6	7	6	12	9	8	10	13	11	10	11	19	12	15	20
30–40°	7	6	4	2	9	10	5	6	12	11	7	6	10	9	12	9
20–30°	7	5	3	2	9	9	5	5	11	10	6	5	3	6	15	8
10–20°	6	9	4	2	6	5	5	5	8	10	6	5	12	24	25	15
0–10°	5	8	6	2	4	5	6	6	6	10	8	6	11	8	8	12

North latitude	$\sigma(\text{div } \mathbf{T}_O)/\sqrt{N}$				$\sigma(\mathbf{T}_A)/\sqrt{N}$†					$\sigma(\mathbf{T}_O)/\sqrt{N}$†			
	DJF	MAM	JJA	SON		DJF	MAM	JJA	SON	DJF	MAM	JJA	SON
80–90°	—	—	—	—	80°N	0.2	0.2	0.1	0.2	0.5	0.3	0.3	0.3
70–80°	—	—	—	—	70°	0.4	0.3	0.1	0.3	0.6	0.3	0.3	0.4
60–70°	25	21	22	25	60°	0.5	0.2	0.2	0.2	0.6	0.4	0.3	0.6
50–60°	27	17	18	18	50°	0.4	0.2	0.3	0.2	0.8	0.6	0.5	0.8
40–50°	23	17	18	23	40°	0.4	0.3	0.3	0.3	1.3	1.0	1.0	1.5
30–40°	16	15	14	11	30°	0.4	0.5	0.2	0.2	1.6	1.4	1.4	1.8
20–30°	12	12	16	10	20°	0.3	0.2	0.1	0.2	1.6	1.2	1.9	2.1
10–20°	14	26	26	16	10°	0.2	0.2	0.1	0.2	1.7	1.1	2.4	2.4
0–10°	12	13	12	13	0°	0.2	0.1	0.2	0.2	1.6	1.3	2.6	2.7

* $N=2$ or 3 for F_{TA}, $N=5$ for div $\mathbf{T}_A$, $N=1$ for S_O, $N=5$ for $\mathbf{T}_A$, and N is unspecified for the residual terms F_{BA}, div $\mathbf{T}_O$, and $\mathbf{T}_O$.

** For F_{BA}, div $\mathbf{T}_O$ and $\mathbf{T}_O$ the standard errors of the mean were estimated using the law of propagation of independent errors:

$$\sigma(F_{BA})/\sqrt{N_4}=[\sigma^2(F_{TA})/N_1+\sigma^2(S_A)/N_2+\sigma^2(\text{div } \mathbf{T}_A)/N_3]^{+\frac{1}{2}}$$

$$\sigma(\text{div } \mathbf{T}_O)/\sqrt{N_6}=[\sigma^2(F_{BA})/N_4+\sigma^2(S_O)/N_5]^{+\frac{1}{2}}$$

$$\sigma(\mathbf{T}_O)/\sqrt{N_6}=\text{(see text for explanation)}$$

where N_1, N_2, N_3, N_4, N_5 and N_6 indicate the number of samples for F_{TA}, S_A, div $\mathbf{T}_A$, F_{BA}, S_O and div $\mathbf{T}_O$, respectively.

† For the transport terms $\mathbf{T}_A$ and $\mathbf{T}_O$, the units are 10^{15} W, instead of W m^{-2}.

APPENDIX B

Sources of Uncertainty

For each term in the atmospheric and terrestrial heat balance equations (7a) and (8a) the uncertainty in the values presented will be discussed.

In the values of F_{TA} certain systematic errors may appear mainly related to the calibration of the sensors, the degradation of the sensors in space, a possible diurnal sampling bias for satellites in sun synchronous orbits, parameterizations applied to some medium resolution sensor data for narrow spectral band sampling, temporal and spatial sampling gaps in each monthly mean, and finally the uncertainty in the value of the solar constant used to compute the net incoming solar radiation.[2] A further source of uncertainty is the natural year-to-year variability that will affect the climatological averages if the number of samples is small. In the present data set, this last uncertainty appears to dominate. Standard errors of the mean ($\sigma N^{-\frac{1}{2}}$) have been computed and are shown in Table 13. The usual interpretation of the standard error of the mean is as follows. Namely, one may expect with 95% confidence that the true value of the quantity in question will lie between the mean value as given in the previous tables plus or minus twice the standard error of the mean. For easy reference, annual mean 95% confidence limits were computed from the standard errors of the mean as presented in Table 13 and were included in the various latitude-month cross sections presented in the main part of the paper. Coming back to the discussion of Table 13, one notices that the standard errors of the mean for F_{TA} are largest in winter at high latitudes and range between 10 and 15 W m^{-2}. At other latitudes typical values are of the order of 5 W m^{-2}.

Errors in S_A appear to be small since the relevant atmospheric temperature and humidity fields are well measured, and do not fluctuate much from year to year within the 1958–1963 period of record. The standard errors of the mean tend to be of the order of 1 W m^{-2} or less, and therefore are not given in Table 13.

[2] In the case of the ESSA 7 data, global net radiative equilibrium was assumed on a daily basis. However, according to a recent study by the present authors and their associates (Ellis *et al.*, 1976) this assumption is not justified, even on a mean monthly basis. Fortunately, it does not appreciably affect the shape of the zonal profiles presented in Table 2, but it will have some effect on the hemispheric mean estimates. Thus, without including the ESSA 7 data the hemispheric averages of net radiational heating from October through March would be −26, −49, −59, −57, −21 and 23 Wm^{-2}, respectively, instead of the actual values given in Table 2 of −27, −57, −70, −62, −32 and 10 W m^{-2}.

The standard errors of the mean of div $\mathbf{T}_A$ were also estimated from the year-to-year differences observed within the 5-year period of record, and are tabulated in Table 13. Some systematic errors associated with poor data coverage over the tropical oceans may affect the transports, especially at low latitudes. However, the computed standard errors are large, and reflect probably for the most part real interannual variability for the different calendar months rather than errors due to unrepresentativeness of the transports. The table shows at polar latitudes for div $\mathbf{T}_A$ typical values of the order of 20 to 30 W m^{-2}, at middle latitudes about 10 W m^{-2}, and at low latitudes about 5 W m^{-2}. The intercomparison of the "error" estimates for F_{TA} and div $\mathbf{T}_A$ seems to indicate that, in spite of rather small imposed year-to-year fluctuations in net radiation at the top, relatively large interannual variations tend to occur in the atmospheric transports. The anomalous atmospheric transports would then have to be compensated "internally," i.e., either by abnormal storage of heat in the oceans or more likely by anomalous oceanic heat transports. At present, this can only be a matter of speculation.

The uncertainty in F_{BA}, computed as a residual, is of course larger than in any of the other components in the atmospheric branch of the energy cycle. Its standard error of the mean in Table 13 was computed from the individual error estimates for F_{TA}, S_A and div $\mathbf{T}_A$ by using the law of propagation of independent errors. Typical values range between 15 and 35 W m^{-2} at high latitudes and are about 10 W m^{-2} or less at low and middle latitudes.

The oceanic heat storage estimates may contain errors due to the lack and/or sparseness of temperature data in certain regions, and also due to the neglect of possible temperature variations below 275 m depth. The first problem does not seem to be too serious in the case of long-term averages, because the data coverage during the different calendar months proved to be rather good. Only when ice is present the data coverage seems insufficient. Thus north of 50°N there are data-sparse regions just east of the continents, and north of 80°N practically no data are available throughout the year. The errors introduced by neglecting the heat storage in the layers below 275 m are difficult to estimate, because the temperature measurements at these levels do not seem good enough to distinguish between noise and real annual variations. On the other hand, there is some evidence (e.g., Fig. 7) that this last problem also is not very serious. The uncertainty could not be measured in the same manner as in the atmospheric case because all data from different years (but for the same calendar month) were treated as one sample. Instead the standard error of the mean was estimated by comparing our 275 m heat storage values with our 137.5 m values, as well as with the 137.5 m storage values based on the Bauer-Robinson (1973) grid point data. The computed standard error of the mean turned out to be generally between 10 and 20 W m^{-2}. Only in the 10–20°N belt were maximum values of 25 W m^{-2} computed.

Again using the law of propagation of independent errors, one can deduce error estimates for the convergence of heat due to oceanic motions obtained as a residual in (8a). Thus the standard errors of the mean were found to range between 15 and 25 W m^{-2}.

Finally, it will be of interest to determine error limits for the computed atmospheric and oceanic transports. Surprisingly enough, the year-to-year variability in the atmospheric fluxes themselves is much smaller than that in the atmospheric flux divergences, at least in a relative sense. Thus the standard errors of the mean are found to be at most 0.5×10^{15} W compared with actual fluxes of almost 5×10^{15} W. The uncertainty in the oceanic transports can be deduced by considering the errors in $\mathbf{T}_A$ at that latitude, together with those in F_{TA} and S_A+S_O integrated over the polar cap bounded by that latitude. Thus, reasonable standard error of the mean estimates for the ocean transports seem to be 1 to 2×10^{15} W in middle and 2 to 3×10^{15} W at low latitudes.

REFERENCES

Aagaard, K., and P. Greisman, 1975: Toward new mass and heat budgets for the Arctic Ocean. *J. Geophys. Res.*, **80**, 3821–3827.

Bauer, R. A., and M. K. Robinson, 1973: Northern Hemisphere numerical atlas. Compass Systems, Inc., San Diego, Calif.

Bryan, K., 1962: Measurements of meridional heat transport by ocean currents. *J. Geophys. Res.*, **67**, 3403–3414.

——, and E. Schroeder, 1960: Seasonal heat storage in the North Atlantic Ocean. *J. Meteor.*, **17**, 670–674.

Budyko, M. I., 1963: *Atlas of the Heat Balance of the Earth.* (In Russian.) Moscow, Globnaia Geofiz. Observ., 69 pp.

Cressman, G. P., 1959: An operational objective analysis scheme. *Mon. Wea. Rev.*, **87**, 367–374.

Ellis, J. S., and T. H. Vonder Haar, 1976: Zonal average earth radiation budget measurements from satellites for climate studies. Atmospheric Science Paper 240, Atmospheric Science Department, Colorado State University, Fort Collins.

——, ——, A. H. Oort and S. Levitus, 1976: The annual variation in the global heat balance of the earth based on new observations. Manuscript in preparation.

Flanders, D. H., and W. L. Smith, 1975: Radiation budget data from the meteorological satellites ITOS 1 and NOAA 1. NOAA Tech. Memo. NESS 72.

Fritz, S., 1958: Seasonal heat storage in the ocean and heating of the atmosphere. *Arch. Meteor. Geophys. Bioklim.*, **A10**, 291–300.

Gabites, J. F., 1950: Seasonal variations in the atmospheric heat balance. Sc.D. thesis, Massachusetts Institute of Technology.

Holland, W. D., and A. Hirschman, 1972: A numerical calculation of the circulation in the North Atlantic Ocean. *J. Phys. Oceanogr.*, **2**, 336–354.

Jung, G. H., 1952: Note on the meridional transport of energy by the oceans. *J. Marine Res.*, **11**, 139–146.

Kukla, G. J., and H. J. Kukla, 1974: Increased surface albedo in the Northern Hemisphere. *Science*, **183**, 709–714.

London, J., 1957: A study of the atmospheric heat balance. Final Report, Contract AF19(122)-165, Dept. Meteor. Oceanogr., New York University, 90 pp.

MacDonald, T. H., 1970: Data reduction processes for spinning flat-plate satellite-borne radiometers. ESSA Technical Report NESC 52.

Maykut, G. A., and N. Untersteiner, 1971: Some results from a time dependent thermodynamic model of sea ice. *J. Geophys. Res.*, **76**, 1550–1575.

Newell, R. E., J. W. Kidson, D. G. Vincent and G. J. Boer, 1974: The general circulation of the tropical atmosphere and interactions with extratropical latitudes, Vol. 2. The MIT Press, Cambridge, Mass., 371 pp. (see pp. 27–33, 58–61).

——, D. G. Vincent, T. G. Dopplick, D. Ferruzza and J. W. Kidson, 1970: The energy balance of the global atmosphere. *The Global Circulation of the Atmosphere.* G. A. Corby, Ed., Royal Meteorological Society, London, England, 42–90.

Niiler, P. P., and W. S. Richardson, 1973: Seasonal variability of the Florida Current. *J. Marine Res.*, **31**, 144–167.

Oort, A. H., 1971: The observed annual cycle in the meridional transport of atmospheric energy. *J. Atmos. Sci.*, **28**, 325–339.

——, and E. M. Rasmusson, 1971: *Atmospheric Circulation Statistics.* NOAA Prof. Paper No. 5, U. S. Government Printing Office, Washington, D. C., 323 pp.

Pattullo, J. G., 1957: The seasonal heat budget of the oceans. Sc.D. thesis, UCLA, 104 pp.

Peixóto, J. P., 1973: Atmospheric vapor flux computations for hydrological purposes. WMO Rept. No. 20, Geneva, Switzerland, 83 pp.

Rasool, S. I., and C. Prabhakara, 1966: Heat budget of the Southern Hemisphere. *Problems of Atmospheric Circulation*, Washington, D. C., Spartan Books, 76–92.

Sellers, W. D., 1965: *Physical Climatology.* The University of Chicago Press, 272 pp.

Vonder Haar, T., and K. J. Hanson, 1969: Absorption of solar radiation in tropical regions. *J. Atmos. Sci.*, **26**, 652–655.

——, and A. H. Oort, 1973: New estimate of annual poleward energy transport by Northern Hemisphere oceans. *J. Phys. Oceanogr.*, **2**, 169–172.

——, and V. Suomi, 1971: Measurements of the earth's radiation budget from satellites during a five-year period. Part I: Extended time and space means. *J. Atmos. Sci.*, **28**, 305–314.

Wetherald, R. T., and S. Manabe, 1972: Response of the joint ocean-atmosphere model to the seasonal variation of the solar radiation. *Mon. Wea. Rev.*, **100**, 42–59.

Wiesnet, D. R., and M. Matson, 1975: Monthly winter snowline variation in the Northern Hemisphere from satellite records, 1966–75. NOAA Tech. Memo. NESS 74, 21 pp.

Wyrtki, K. O., 1965: The average annual heat balance of the North Pacific Ocean and its relation to ocean circulation. *J. Geophys. Res.*, **70**, 4547–4559.